Nucleosome Structure Modulates Benzo[*a*]pyrenediol Epoxide Adduct Formation†

Brian D. Thrall,‡ David B. Mann,‡,§ Michael J. Smerdon,§ and David L. Springer*,‡

Biology and Chemistry Department, Pacific Northwest Laboratory, P7-56, Box 999, Richland, Washington 99352, and Department of Biochemistry and Biophysics, Washington State University, Pullman, Washington 99164

Received August 31, 1993; Revised Manuscript Received December 15, 1993®

ABSTRACT: We have studied the binding of a chemical carcinogen to DNA reconstituted with histone octamers to determine the effect that nucleosome structure has on covalent adduct formation. Reconstitution of a plasmid containing the somatic 5S rRNA gene from *Xenopus borealis* resulted in characteristic nucleosome structure, as determined by micrococcal nuclease digestion, shifted migration in agarose gels, and hydroxyl radical footprinting. Formation of covalent adducts by benzo[*a*]pyrenediol epoxide (BPDE) occurred initially at a slower rate in reconstituted DNA than in naked plasmid, but after 2 h the total adduction levels (adducts/plasmid) were equal in both samples. Analysis of adduction at the sequence level by primer extension indicated that, after a 2-h BPDE reaction, the degree of adduction within the 5S rRNA nucleosome was suppressed by approximately 50% compared to naked DNA. The rotational setting of the guanines on the helix did not explain the level of adduction observed, since guanines in close proximity to the histone core were equally susceptible to adduction as guanines on the outer nucleosome surface. At early reaction times with BPDE, however, sequences near the 5S nucleosome dyad, where known modulations in the minor groove width occur, were the least susceptible to adduction. These results indicate that the structural features of DNA assembled into nucleosomes contribute to the susceptibility of the DNA to modification by BPDE.

Benzo[*a*]pyrene-7,8-diol 9,10-epoxide (BPDE[1]), the ultimate carcinogenic metabolite of benzo[*a*]pyrene, covalently binds to DNA predominantly at guanine residues (Straub et al., 1977). Covalent adduct formation by BPDE interferes with a number of cellular processes, including DNA replication and transcription, and is thought to be a critical event in tumor initiation. The primary target of covalent modification is through trans addition of the diol epoxide (C10) to the exocyclic (N2) amine group of guanine [Straub et al., 1977; reviewed in Graslund and Jernstrom (1989)]. Although the precise steps in covalent adduct formation are not clear, it is hypothesized that an initial noncovalent intercalation complex is involved (Meehan et al., 1982; Geacintov et al., 1986).

The majority of DNA in eukaryotic cells is closely associated with histone proteins, forming the building block of higher order chromatin structure, the nucleosome. Thus, an accurate understanding of carcinogen binding to DNA must consider the role of nucleosome structure. In the nucleosome, contact points exist between the DNA and histone cores approximately every 10 bp (Arents et al., 1991), and histones H3 and H4 make contact with the DNA within 30 bp of either side of the center (dyad) of the nucleosome (Pruss & Wolffe, 1993). In addition, the helical periodicity of DNA varies throughout the nucleosome, with the central three turns of the helix having a periodicity of 10.7 bp and the outer turns having 10.0-bp periodicity (Hayes et al., 1990, 1991). Thus, it is conceivable that the periodicity of nucleosomal DNA and interaction points with histone proteins would alter the susceptibility of particular bases to carcinogen damage. Indeed, studies by Gale et al. (1987) showed that UV-induced pyrimidine dimer formation in nucleosomes was not uniform, but was maximal at bases that were farthest from the histone core, resulting in an average 10.3-bp repeat pattern of damage.

Studies with the bulky aflatoxin-derived adduct (Moyer et al., 1989) also demonstrated that binding was suppressed up to 2.4-fold in nucleosomal DNA compared to naked DNA, again setting a precedent for examining the influence of nucleosome structure on covalent binding by bulky carcinogens. Obi et al. (1986) showed that BPDE preferentially binds to DNA in "active" chromatin compared to bulk chromatin, presumably due to differences in chromatin structure. Others (MacLeod et al., 1989) have reported that naked and nucleosomal DNA from genomic sources are bound to similar degrees by BPDE; however, both the rate of adduction and types of adducts produced varied. Binding of BPDE to DNA is also influenced by DNA sequence (Boles & Hogan, 1984; Reardon et al., 1989; Dittrich & Krugh, 1991; Thrall et al., 1992), with preference for modification of guanines flanked by 3′-guanines. However, the influence of the nucleosome on the sequence specificity of BPDE binding is not known. To explore these questions, we used a plasmid containing the 5S rRNA gene, which forms a highly positioned nucleosome (Rhodes, 1985), to reconstitute nucleosome particles *in vitro* and to examine the effect of nucleosome assembly on the sequence-related patterns of BPDE modification.

MATERIALS AND METHODS

Plasmid DNA and Other Materials. Plasmid pGEM-5S (3126 bp), containing the somatic 5S rRNA gene from *Xenopus borealis* subcloned from plasmid pXP-14.4 (Peterson et al., 1980), has been previously described (Thrall et al., 1992). The plasmid was isolated from JM109 bacteria by the large-scale alkaline lysis procedure (Maniatis et al., 1982). Micrococcal nuclease was purchased from Worthington Biochemical (Freehold, NJ). Sequenase Version 2.0 (cloned

† This research was supported by the U.S. Department of Energy under contract DE-AC06-76RLO 1830 (D.L.S.) and NIH Grant ES02614 (M.J.S.).

* Author to whom correspondence should be addressed.
‡ Pacific Northwest Laboratory.
§ Washington State University.

® Abstract published in *Advance ACS Abstracts,* February 1, 1994.

[1] Abbreviations: BPDE, (±)-*anti*-benzo[*a*]pyrene-7,8-diol 9,10-epoxide; bp, base pair.

0006-2960/94/0433-2210$04.50/0

T7 DNA polymerase) and T4 polynucleotide kinase were from U.S. Biochemical (Cleveland, OH). Radiolabeled nucleotides were from New England Nuclear, Dupont (Wilmington, DE). Tritium-labeled (±)-*anti*-7*r*,8*t*-dihydroxy-9,10*t*-oxy-7,8,9,10-tetrahydrobenzo[*a*]pyrene was purchased from the Cancer Research Program of the National Cancer Institute, Division of Cancer Cause and Prevention (Bethesda, MD), and was stored in a solution of 19:1 tetrahydrofuran/triethylamine. All other materials were reagent grade or better.

Reconstitution and Enzymatic Characterization of pGEM-5S. Core histones were isolated from 10 mL of packed chicken erythrocytes using hydroxyapatite, as described by Stein (1989). The isolated histones were concentrated using Centricon 10 ultrafiltration cartridges (Amicon, Beverly, MA) to a final concentration of approximately 0.5 mg/mL, and the integrity of the histones was checked routinely by SDS–polyacrylamide gel electrophoresis. The histone concentration was determined spectrophotometrically both by the method of Waddell (1956) and by monitoring the absorbance at 275.5 nm using the average extinction coefficient for the core histones (D'Anna & Isenberg, 1974). The mean value for these independent concentration measurements was used in these experiments.

Reconstitution of plasmid DNA was accomplished by stepwise dialysis. Histone core particles and plasmid were mixed in a 10:1 molar ratio (histone cores/DNA) in buffer containing 1 M NaCl, 20 mM Tris Cl (pH 7.2), 0.2 mM EDTA, and 0.1 mM phenylmethanesulfonyl fluoride. The sample was dialyzed at 4 °C in a Spectrapore MWCO 12000–15000 dialysis membrane for 8 h each in buffers containing 0.8, 0.1, and 0.05 M NaCl concentrations. Analysis of reconstituted samples was by electrophoresis in 1% agarose gels in buffer containing 9 mM Tris, 9 mM boric acid, and 0.2 mM EDTA (1× TBE). Digestions with micrococcal nuclease were run at 37 °C using the final reconstitution buffer and 1 mM $CaCl_2$ with 250 units/mL micrococcal nuclease. Hydroxyl radical footprinting was accomplished using restriction fragments containing the 5S rRNA gene, as described by Tullius et al. (1987).

Adduction of DNA with [^{3}H]-anti-BPDE. Naked and reconstituted plasmid DNA (250 μg/mL) were incubated with [^{3}H]-(±)-*anti*-BPDE in 10 mM Tris Cl (pH 7.2), 1 mM EDTA (TE), and 50 mM NaCl for 5–120 min. Typically, we used 10 μM BPDE in these experiments, which resulted in approximately 3 adducts/plasmid after a 2-h incubation. In all cases, the solvent (THF/TEA, 19:1) concentration used was less than 5% of the total reaction volume and was included in the control (naked) DNA samples. For the time course experiment, the reactions were stopped at each time point by rapid extraction with an equal volume of phenol/chloroform/isoamyl alcohol (P:C:I = 25:24:1), followed by extraction with chloroform/isoamyl alcohol (C:I = 24:1) and ethanol precipitation. The samples were centrifuged (12000*g*, 15 min), lyophilized, and resuspended in 100 μL of TE buffer. The protein was further removed by digestion with 100 μg/mL proteinase K for 2 h (37 °C), and two additional extractions were performed with P/C/I and C/I, followed by ethanol precipitation. The final pellet was resuspended in TE buffer, and the DNA concentration was determined by UV absorbance. The amount of radioactivity copurifying with the DNA was determined after scintillation analysis in 20 mL of Formula 989 scintillation cocktail (Dupont, Boston, MA) using a Beckman Model LS9000 liquid scintillation counter, and adduction levels were calculated on the basis of radioactivity measurements and UV estimates of DNA concentration.

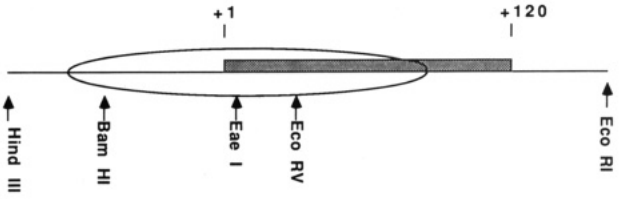

FIGURE 1: Position of the 5S nucleosome and unique restriction sites within the 5S rRNA gene. The somatic 5S rRNA gene from *Xenopus borealis* (shaded) forms a single nucleosome (oval), which is reported to be positioned with the dyad approximately over the transcriptional start of the 5S gene. The locations of unique restriction sites inside and outside of the nucleosome are shown by arrows.

Primer Extension Analysis. The pattern of BPDE modification on naked and reconstituted pGEM-5S was analyzed by primer extension methods using Sequenase. For these reactions, 150 ng of primer was 5′-end-labeled with [γ-^{32}P]-ATP using T4 polynucleotide kinase by standard procedures and annealed with 2 μg of plasmid. Extension reactions contained 200 μM deoxynucleotide triphosphates in the supplied reaction buffer and were carried out at 37 °C for 5 min. For DNA sequence references, standard dideoxynucleotide triphosphate sequencing reactions were run according to the manufacturer's instructions. All samples were separated on 10% denaturing polyacrylamide gels and exposed to Kodak XAR-5 film for 12–24 h. Densitometric analysis of the autoradiographs was performed using a Zeineh Model SL/2D laser densitometer in the log measuring mode.

RESULTS

Reconstitution of Plasmid DNA. A schematic representation of the location of the 5S nucleosome relative to the 5S rRNA gene, as well as the locations of unique restriction enzyme sites, is shown in Figure 1. The 5S nucleosome is reported to form with the dyad of the nucleosome positioned at approximately the transcriptional start of the 5S rRNA gene (Rhodes, 1985). Reconstitution of plasmid pGEM-5S into nucleosomal DNA was accomplished using isolated histone core octamers from chicken erythrocytes. Characterization of the histone octamers by both HPLC and SDS–polyacrylamide gel electrophoresis indicated that the isolated histones were intact and that histones H1 and H5 were absent (not shown). Agarose gel analysis of pGEM-5S reconstituted at a histone (octamer):DNA molar ratio of 10:1 is shown in Figure 2. Higher histone:DNA ratios were not used since an insoluble precipitate formed during the reconstitution procedure. Compared to the sham reconstituted control, association of the histone octamers retarded the migration of reconstituted DNA in agarose (Figure 2A, lanes 2 and 3). The normal rate of migration was restored in the reconstituted sample after proteinase K digestion (Figure 2A, lane 4), demonstrating that the plasmid remained supercoiled throughout the reconstitution procedures. To check for the presence of *bona fide* nucleosomes, the reconstituted sample was digested with micrococcal nuclease. A time course for micrococcal nuclease digestion (Figure 2B) revealed a characteristic ladder of DNA fragments of approximately 146-bp repeats, the length of nucleosome core DNA. The earliest time points for micrococcal digestion showed DNA fragments approximately 750 bp in length, indicating the presence of a minimum of five nucleosomes on the plasmid.

To determine whether a nucleosome is present in the 5S gene of the plasmid pGEM-5S, restriction digestion analysis was performed (Figure 2C). Under conditions that allowed complete linearization of the naked plasmid, reconstituted

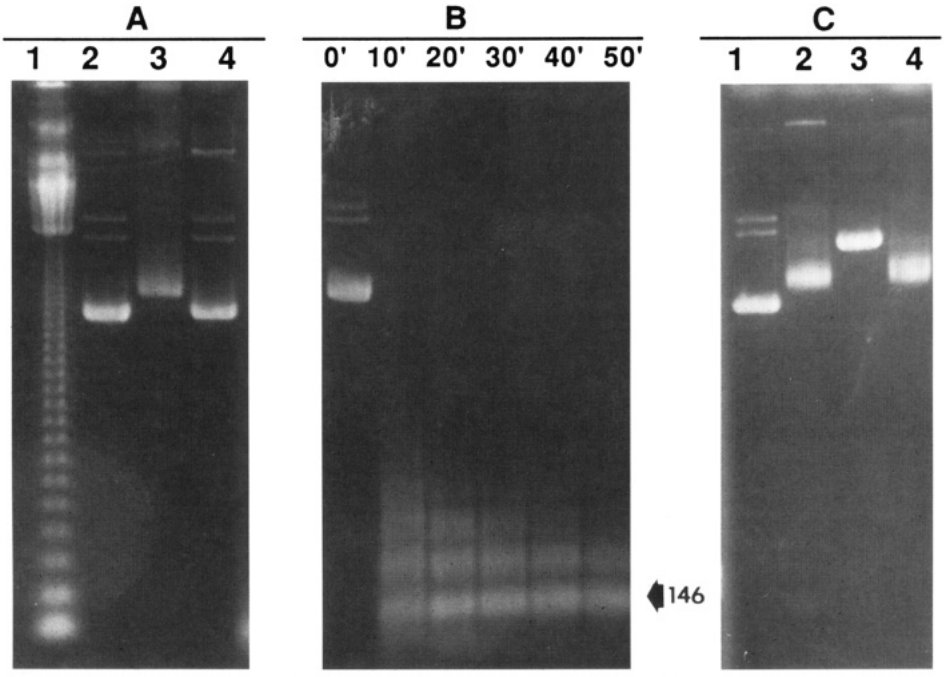

FIGURE 2: Agarose electrophoresis and micrococcal nuclease digestion of reconstituted pGEM-5S. (A) Migration of reconstituted DNA in 1% agarose: (1) 123-bp ladder; (2) sham reconstituted pGEM-5S (primarily supercoiled); (3) reconstituted pGEM-5S; (4) reconstituted sample after proteinase K digestion. (B) Time course for micrococcal nuclease digestion. Reconstituted plasmid was digested with 250 units/mL micrococcal nuclease for 0–50 min, followed by extraction with phenol/chloroform (24:1) and electrophoresis on 1% agarose. (C) Digestion of naked and reconstituted pGEM-5S with *Eco*RV: (1) naked, nondigested; (2) reconstituted, nondigested; (3) naked, digested; (4) reconstituted, digested.

pGEM-5S was completely protected from digestion with *Eco*RV, which cuts within the 5S nucleosome region (see Figure 1), strong evidence for the presence of a nucleosome at the 5S sequence within the plasmid. Since there was little indication of partial digestion of the reconstituted sample with *Eco*RV, it appeared that the majority of the plasmid molecules contain a nucleosome within the 5S gene. Similar results were found with other enzymes that cut within the 5S gene, including *Eae*I and *Bam*HI (not shown). In addition, we have found partial digestion with *Hin*dIII in reconstituted DNA (not shown), which digests at a single site 87 bp upstream from the start of the 5S gene. This is in agreement with the proposed positioning of the 5S nucleosome, since the *Hin*dIII site would be predicted to be outside of this nucleosome (Rhodes, 1985; Pruss & Wolffe, 1993). However, partial digestion with *Hin*dIII could also reflect the formation of other nucleosomes adjacent to the 5S nucleosome.

To further confirm the presence of a nucleosome in the 5S rRNA gene, as well as determine the positions of the guanines on the DNA helix within the nucleosome (rotational setting), hydroxyl radical footprinting was performed on a 300-bp restriction fragment containing the 5S rRNA gene. The results for the noncoding strand are shown in Figure 3. Cleavage of nucleosomal DNA by hydroxyl radicals is known to occur more intensely in regions where the minor groove of the DNA is facing away from the histone octamer (Tullius et al., 1987; Hayes et al., 1990). In these experiments, hydroxyl radical cleavage of reconstituted DNA resulted in a characteristic pattern of protection approximately every 10 bp, while cleavage of the naked DNA sample was random. Analysis of the positions of most intense cleavage revealed a strong cut site at about the start of the 5S gene in both the naked and reconstituted samples. Since this occurred in both naked and reconstituted DNA, we interpret this to be a native structural characteristic of the DNA. Within the approximately 2-base resolution of these experiments, these results reveal that both the translational position and the rotational setting of the 5S nucleosome concur with those reported by Hayes et al. (1991), with peak intensities corresponding to bases −15, −5, +6, +17, +27, +37, +47, and +57 surrounding the presumed position of the nucleosomal dyad (base +10) (Pruss & Wolffe, 1993).

Adduction of Reconstituted pGEM-5S with BPDE. The influence of nucleosome structure on the rate of total covalent adduct formation by 10 μM BPDE was determined using liquid scintillation analysis. The results shown in Figure 4 are from one experiment, which was repeated several times with similar results. Covalent binding of BPDE to the DNA initially proceeded rapidly and then decreased, such that after 60 min the majority of the adduction had occurred. We attribute the decreased rate of adduction after 60 min to a decrease in the concentration of BPDE in the reaction, presumably the result of hydrolysis of the diol epoxide to tetraol. Reconstituted DNA showed a time course of adduction similar to that of naked DNA; however, the initial rate of covalent adduct formation in the reconstituted sample was suppressed compared to that in the naked DNA. At early time points (5–30 min), the number of adducts/plasmid was approximately 22–30% less in the nucleosomal samples than in the naked DNA. After a 30-min incubation, the naked DNA had an average of 2.7 adducts/plasmid compared to 1.8 in the reconstituted sample. However, by 60 min, the total adduction levels of both samples were approximately equal and remained equal through 120 min, where the final adduction levels were 3.1 and 3.2 for naked and reconstituted plasmids, respectively.

To determine the effect of nucleosome structure on the sequence-specific binding patterns of BPDE within the 5S nucleosome, we used blockage of a DNA polymerase (Sequenase) during primer extension as an indication of adduction patterns (Thrall et al., 1992). The results obtained for the noncoding strand of the 5S gene region in samples reacted with BPDE for 120 min are shown in Figure 5. In these samples, the total adduction levels were similar, with approximately 3 adducts/plasmid. Nonadducted DNA did not

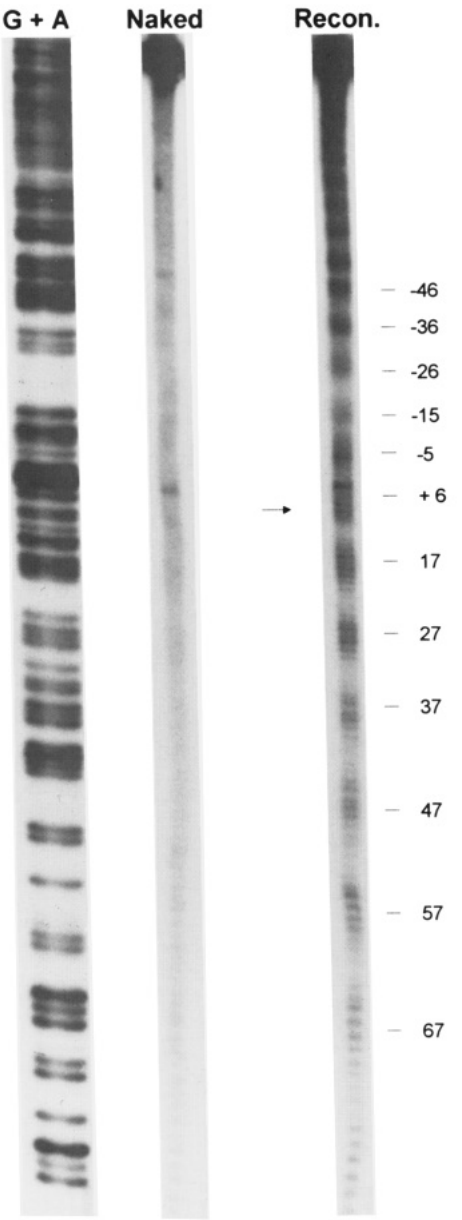

FIGURE 3: Hydroxyl radical footprinting of the 5S nucleosome. A 300-bp restriction fragment containing the 5S rRNA gene from pGEM-5S was labeled with [^{32}P]ATP using T4 polynucleotide kinase, and hydroxyl radical footprinting was performed as described by Tullius et al. (1987). The samples were electrophoresed on 8% denaturing polyacrylamide gels and exposed to Amersham Hyperfilm-Mp. A G+A sequencing lane for the noncoding strand was used to determine the positions of most intense cleavage with respect to the start of the 5S gene (+1). The arrow indicates the position of the nucleosome dyad, as reported by Pruss and Wolffe (1993).

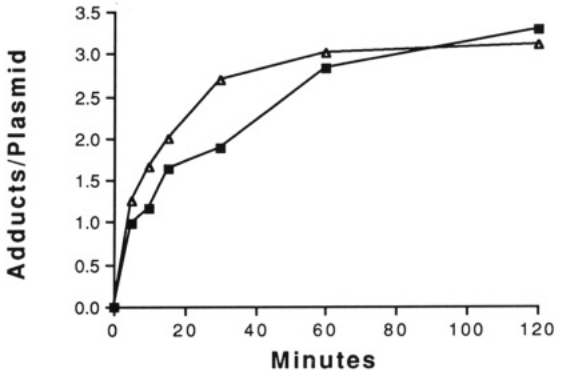

FIGURE 4: Time course of BPDE adduct formation on naked and reconstituted pGEM-5S. Naked (△) and reconstituted (■) pGEM-5S (250 μg/mL) were incubated with 10 μM [^{3}H]-*anti*-BPDE for 0–120 min in the final reconstitution buffer. After removal of the protein and unbound reaction products by digestion with proteinase K and extraction with phenol/chloroform/isoamyl alcohol (25:25:1), binding levels were determined by liquid scintillation analysis and UV absorption (260 nm) of total DNA. The data plotted are from one experiment that was repeated three times with similar results.

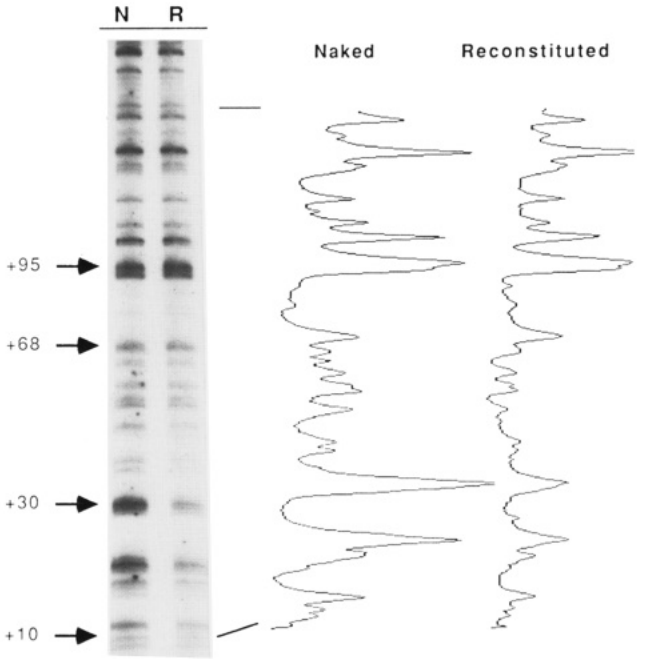

FIGURE 5: Analysis of binding within the 5S nucleosome by primer extension. Analysis of BPDE adduct formation after a 120-min reaction with either naked (N) or reconstituted (R) DNA was carried out by primer extension, as described in Materials and Methods. The numbering refers to guanine position relative to the start of the 5S gene (+1). Densitometric scans of the lanes are shown to the right of the figure. The 3′-end of the nucleosome begins at approximately base +78.

produce polymerase blockage in these experiments, whereas comparison of the bands produced by primer extension of the adducted samples with dideoxy sequencing ladders resulted in polymerase blockage at one base prior to guanines (data not shown). Densitometric analysis of these bands (Figure 5) revealed that, in regions outside the 3′-edge of the nucleosome (>78 bp), the relative degree and pattern of polymerase blockage were similar in both naked and nucleosomal DNA. However, within the 5S nucleosome, the degree of polymerase blockage, and thus the amount of adduction, was suppressed in the reconstituted sample by approximately 50%. This pattern of BPDE binding was consistent with the position of the 5S nucleosome (Rhodes, 1985), since the positions in which adduct formation was suppressed corresponded with the 3′-edge of the nucleosome. These results demonstrate that nucleosome structure inhibits BPDE binding and provide additional evidence for the presence of a positioned 5S nucleosome in the plasmid.

To determine whether there were differences in susceptibility to BPDE modification within the nucleosome, primer extension was conducted on naked and reconstituted samples that were reacted with BPDE for varying times. The degree of protection by the nucleosome (expressed as percent adduction for the equivalent sites in naked DNA) relative to the position of the guanine (distance from the nucleosome dyad) is shown in Figure 6. Samples that were reacted for 120 min with BPDE showed a 50–60% decrease in binding throughout the nucleosome, and at the edge of the nucleosome (see arrow in Figure 6) the binding level approached that of naked DNA.

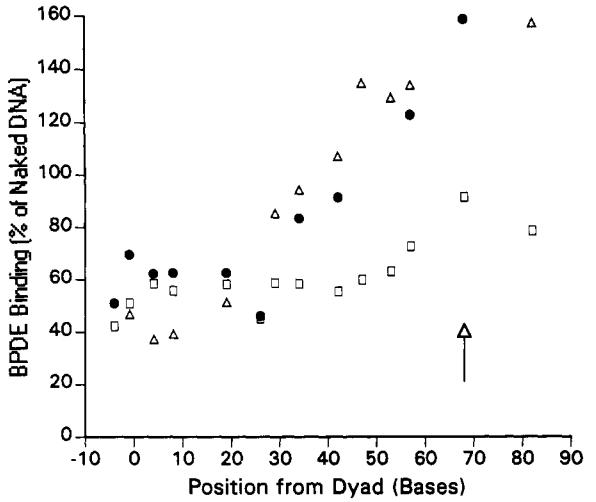

FIGURE 6: Relationship between reaction time and region of the nucleosome. Samples that were reacted with BPDE for varying times were analyzed by primer extension, as shown in Figure 5. The degree of inhibition of binding at individual guanines within the nucleosome, expressed as a percentage of the corresponding site in naked DNA, is plotted versus the position of the guanine in samples reacted with BPDE for 15 (●), 30 (△), or 120 min (□). The arrow indicates the approximate position of the 3′-edge of the nucleosome.

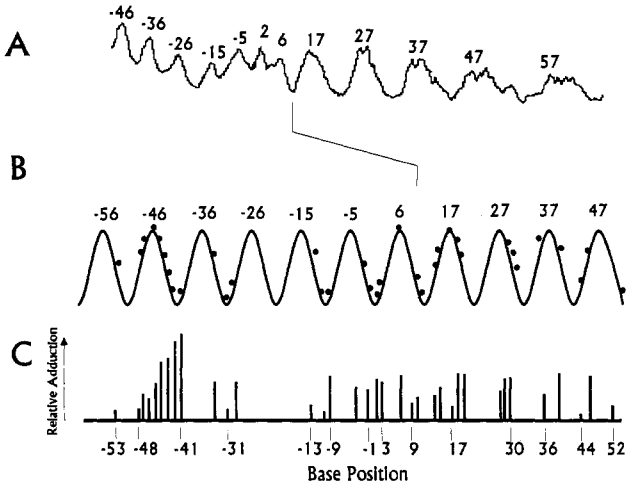

FIGURE 7: Comparison of rotational setting and BPDE binding in reconstituted pGEM-5S. The rotational setting of the guanines and its relationship to adduct formation within the 5S nucleosome were deduced using hydroxyl radical footprinting and primer extension analysis. A shows a densitometric scan of the hydroxyl radical footprint of the reconstituted 5S gene. B is a graphic depiction of the position of the guanines (dots) relative to the DNA helix on the noncoding strand. The position of the dyad corresponds to that reported by Pruss and Wolffe (1993). The peaks of the helix in B represent positions where the minor groove is facing away from the histone cores, whereas the valleys are positions nearest the histone cores. C shows the adduction by BPDE (after a 120-min reaction) at the individual guanines represented in B, relative to the first guanine in the 5S gene (base 2). Note that the *x*-axis in C is not linear and corresponds to the positions of the guanines in B.

In the 15- and 30-min reaction samples, adduct formation in the reconstituted sample was also suppressed. However, the suppression of binding in these samples was progressively greater near the dyad of the nucleosome compared to the fringe. Surprisingly, in the 15- and 30-min samples, the adduction levels on the fringe of the nucleosome were greater than the naked DNA in this experiment.

We hypothesized that the guanines closest to the histone cores would have the least potential for adduction due to steric hindrance. Therefore, a comparison of the positions of the guanines on the DNA helix within the nucleosome and the relative BPDE binding was performed (Figure 7). The positions of the guanines were deduced from the intensity of cleavage by hydroxyl radicals, whereas the relative degree of BPDE binding was determined by primer extension. Within the resolution of the hydroxyl radical footprinting data, we do not find a correlation between the average adduction of guanines and the sensitivity of the guanines to cleavage by hydroxyl radicals. For example, a region of eight consecutive guanines (Figure 7C, bases −41 to −48) showed a bias for greater adduction of the 5′-guanines, yet these guanines appear to be nearest the histone cores. Similar inconsistencies between adduction level and rotational setting occur throughout the 5S nucleosome, and in general there is no apparent correlation between the position of the guanine relative to the histone cores and the frequency for covalent adduct formation.

Within a local sequence context, however, covalent binding of BPDE to a particular guanine is significantly influenced by the flanking bases. For example, the potential for a particular guanine to be modified by BPDE is enhanced by the presence of 3′-flanking guanines (Said & Shank, 1991; Thrall et al., 1992). The pattern of adduction in the poly (dG8) region (Figure 7C, bases −41 to −48) observed in nucleosomal DNA in this study also demonstrates this nearest-neighbor effect and is nearly identical to patterns we have previously reported for this same sequence in naked DNA [i.e., see Figure 5 in Thrall et al. (1992), bases 58–65]. Thus, on a local sequence scale, the nearest-neighbor effects on BPDE binding are not significantly altered within the nucleosome.

DISCUSSION

We have used the somatic *X. borealis* 5S rRNA gene in a plasmid model to determine the influence of nucleosome structure on the formation of covalent adducts by the bulky carcinogen, BPDE. The 5S rRNA gene was chosen because nucleosomes assemble on this gene in a fixed translational position (Rhodes, 1985). Hydroxyl radical footprinting (Figure 3) of a restriction fragment containing the 5S gene indicated that the rotational setting of the 5S nucleosome was consistent with previous reports of the *X. borealis* 5S nucleosome (Rhodes, 1985; Hayes et al., 1991). The results of digestion of pGEM-5S with micrococcal nuclease, which preferentially digests linker DNA, also showed the presence of nucleosome structure on the reconstituted plasmid. Restriction digestion analysis indicated that the cut sites within the 5S rRNA gene in pGEM-5S were completely protected in the reconstituted sample, under conditions in which the naked DNA was completely linearized. We take this as additional evidence for the presence of a nucleosome in the 5S gene of reconstituted pGEM-5S.

The initial rates of total BPDE modification were decreased by 20–30% in the reconstituted samples compared to naked plasmid. At the histone octamer:DNA ratios used in this study (10:1), a maximum of 50% of the base pairs within the plasmid could be associated with histones, since the linear size of the plasmid (3126 bp) could conceivably support 20 nucleosomes. Thus, the 20–30% decrease in BPDE binding determined by liquid scintillation analysis is an underestimate of the amount of protection afforded to the DNA within individual nucleosomes. The true degree of protection was apparent when BPDE adduction levels were measured at the DNA sequence level within the 5S nucleosome, using primer extension methods. Quantitation of the bands produced by polymerase blockage indicated that BPDE binding was suppressed by 50–60% within the 5S nucleosome. This degree

of protection is similar to that observed for aflatoxin binding to nucleosomal DNA (Moyer et al., 1989).

By examining the pattern of binding at early time points during the reaction with BPDE, it was apparent that the sequences surrounding the dyad of the 5S nucleosome were the least susceptible to covalent binding. Since the majority of BPDE adducts are thought to lie within the minor groove, these results suggest that the minor groove is less accessible near the dyad than on the fringe of the nucleosome. Aflatoxin binding to nucleosomal DNA is restricted within the central 100 bases of the nucleosome (Moyer et al., 1989); similarly, the formation of pyrimidine dimers from UV irradiation is lowest in the region of the dyad of the nucleosome (Gale et al., 1987; Gale & Smerdon, 1988). Hydroxyl radical footprinting studies have shown that the average helical repeat of DNA in the 5S nucleosome is 10.18 bp (Hayes et al., 1990). However, the central 30 bp of DNA in the 5S nucleosome is overwound to a periodicity of 10.7 bp, while the DNA outside this region have a 10.0-bp periodicity (Hayes et al., 1991). This overwinding is consistent with a narrowing of the minor groove of the DNA around the nucleosomal dyad, which may be important to the formation of BPDE adducts.

The sequences surrounding the dyad of the nucleosome are also thought to contain bends which contribute to the positioning of the histone octamer [reviewed in Thoma (1992)], and these structural elements may also be important to DNA adduct formation. Interestingly, we found enhanced BPDE binding after early reaction times in regions immediately outside the 5S nucleosome. Since the positions and relative mobilities of other nucleosomes on the plasmid are not known, we are unable to determine whether enhancement of BPDE binding at the edges of nucleosomes is a general characteristic among all nucleosomes. However, nucleosomes can induce bending of linker DNA (Yao et al., 1991), even in the absence of histone H1, and this may affect the level of BPDE binding. Studies are currently underway to determine whether these patterns of BPDE binding are found in other nucleosome systems.

Although the precise steps in the binding of BPDE to DNA are not understood, it is hypothesized that an initial intercalation complex may precede covalent bond formation (Meehan et al., 1982; Geacintov, 1986). In the simplest model of binding proposed by Geacintov (1986), BPDE forms an initial noncovalent intercalation complex, which may either be detoxified by hydrolysis to tetraol or proceed to form covalent adducts. Thus, the overall rate of covalent adduct formation is dependent on several competing parameters, including the rates of formation and removal of the initial intercalation complex as well as of hydrolysis of BPDE. Studies by McMurray and van Holde (1991) have shown that ethidium bromide forms intercalative complexes with nucleosomes more rapidly near the ends than near the dyad regions, which is consistent with the results of this study. MacLeod et al. (1989) demonstrated that hydrolysis of BPDE was inhibited by approximately 30-fold in genomic nucleosomes compared to salmon sperm DNA. Thus, the overall suppression of BPDE binding within the nucleosome likely is not due to an increased rate of hydrolysis.

In addition, spectrophotometric studies using the nonreactive benzo[*a*]pyrene-9,10-diol (BPD) showed a 30-fold weaker association of BPD with core particles compared to purified DNA (MacLeod et al., 1989), consistent with a decreased accessibility of BPD with binding sites in the nucleosome. Our binding results, as well as studies of variations in minor groove widths throughout the nucleosome (Hayes et al. 1991; Richmond et al., 1984), are compatible with the notion that the formation of an initial intercalation complex is limiting in the nucleosome, especially at sequences surrounding the dyad. However, our results do not rule out the possibility that local variations in the rate of hydrolysis of BPDE also exist within the nucleosome, which could contribute to the patterns of binding we have observed.

Comparison of the degree of BPDE binding by primer extension with the results obtained by hydroxyl radical footprinting methods showed that the degree of binding did not strongly correlate with the positions of the guanines on the DNA helix. For as yet unknown reasons, this finding contrasts with results found for pyrimidine dimers in genomic nucleosomes (Gale et al., 1987; Gale & Smerdon, 1988). Damage to nucleosomes by UV shows 10.3-bp periodicity, possibly due to the bending of the DNA helix farthest from the histone core (Pehrson & Cohen, 1992). Formation of pyrimidine dimers requires significant perturbation of the DNA helix (Rao et al., 1984; Pearlman et al., 1985), unlike adduct formation by BPDE, which results in minimal perturbation in the helix (Cosman et al., 1992). Thus, damage to bases near the histone–DNA interface may be energetically more favorable with BPDE than with UV. However, NMR and energy minimization studies (Cosman et al., 1992) suggest that the major adduct structure from BPDE does require a widening of the minor groove. For this widening to occur without significant energy input, it may be that normal thermodynamic fluctuations in minor groove widths are required for the formation of an initial BPDE–DNA complex. Possibly, histone cores do not limit access of BPDE to the minor groove of the DNA, but rather restrict the thermodynamic flexibility of the minor groove and therefore inhibit the formation of the initial BPDE–DNA complex which leads to covalent binding.

Although additional studies are required to discern the mechanisms involved, the patterns of adduction observed in this study correlate with known structural variations of the DNA within the 5S nucleosome and with the proposed mechanisms of BPDE binding. Future studies to determine the sites of adduction and enzymatic processing, as well as the role of the nucleosome structure of critical genes involved in tumor initiation, will be particularly important.

REFERENCES

Arents, G., Burlingame, R. W., Wang, B. W., Love, W. E., & Moudrianakis, E. N. (1991) *Proc. Natl. Acad. Sci. U.S.A. 88*, 10148–10152.

Boles, T. C., & Hogan, M. E. (1984) *Proc. Natl. Acad. Sci. U.S.A. 81*, 5623–5627.

Cosman, M., de los Santos, C., Fiala, R., Hingerty, B. E., Singh, S. B., Ibanez, V., Margulis, L. A., Live, D., Geacintov, N. E., Broyde, S., & Patel, D. J. (1992) *Proc. Natl. Acad. Sci. U.S.A. 89*, 1914–1918.

D'Anna, J. A., & Isenberg, I. (1974) *Biochemistry 13*, 4992–4997.

Dittrich, K. A., & Krugh, T. R. (1991) *Chem. Res. Toxicol. 4*, 270–276.

Gale, J. M., & Smerdon, M. J. (1988) *Biochemistry 27*, 7197–7205.

Gale, J. M., Nissen, K. A., & Smerdon, M. J. (1987) *Proc. Natl. Acad. Sci. U.S.A. 84*, 6644–6648.

Geacintov, N. E. (1986) *Carcinogenesis 7*, 759–766.

Graslund, A., & Jernstrom, B. (1989) *Q. Rev. Biophys. 22*, 1–37.

Hayes, J. J., Tullius, T. D., & Wolffe, A. P. (1990) *Proc. Natl. Acad. Sci. U.S.A. 87*, 7405–7409.

Hayes, J. J., Clark, D. J., & Wolffe, A. P. (1991) *Proc. Natl. Acad. Sci. U.S.A. 88*, 6829–6833.

MacLeod, M. C., Smith, B., & Kao Lew, L. (1989) *Mol. Carcinog. 1*, 245–252.
Maniatis, T., Fritsch, E. F., & Sambrook, J. (1982) in *Molecular Cloning: A Laboratory Manual*, Cold Spring Harbor Laboratory Press, Cold Spring Harbor, NY.
McMurray, C. T., & van Holde, K. E. (1991) *Biochemistry 30*, 5631–5643.
Meehan, T., Gamper, H., & Becker, J. F. (1982) *J. Biol. Chem. 257*, 10479–10485.
Moyer, R., Marien, K., van Holde, K., & Bailey, G. (1989) *J. Biol. Chem. 264*, 12226–12231.
Obi, F. O., Ryan, A. J., & Billet, M. A. (1986) *Carcinogenesis 7*, 907–914.
Pearlman, D. A., Holbrook, S. R., Pirkle, D. H., & Kim, S.-H. (1985) *Science 227*, 1304–1308.
Pehrson, J. R., & Cohen, L. H. (1992) *Nucleic Acids Res. 20*, 1321–1324.
Peterson, R. C., Doering, J. L., & Brown, D. D. (1980) *Cell 20*, 131–141.
Pruss, D., & Wolffe, A. P. (1993) *Biochemistry 32*, 6810–6814.
Rao, S. N., Keepers, J. W., & Kollman, P. (1984) *Nucleic Acids Res. 12*, 4789–4807.
Reardon, D. B., Bigger, A. H., Strandberg, J., Yagi, H., Jerina, D. M., & Dipple, A. (1989) *Chem. Res. Toxicol. 2*, 12–14.
Rhodes, D. (1985) *EMBO J. 4*, 3473–3482.
Richmond, T. J., Finch, J. T., Rushton, B., Rhodes, D., & Klug, A. (1984) *Nature 311*, 532–537.
Said, B., & Shank, R. C. (1991) *Nucleic Acids Res. 19*, 1311–1316.
Stein, A. (1989) *Methods Enzymol. 170*, 585–603.
Straub, K. M., Meehan, T., Burlingame, A. L., & Calvin, M. (1977) *Proc. Natl. Acad. Sci. U.S.A. 74*, 5285–5289.
Thoma, F. (1992) *Biochim. Biophys. Acta 1130*, 1–19.
Thrall, B. D., Mann, D. B., Smerdon, M. J., & Springer, D. L. (1992) *Carcinogenesis 13*, 1529–1534.
Tullius, T. D., Dombroski, B. A., Churchill, M. E. A., & Kam, L. (1987) *Methods Enzymol. 155*, 537–558.
Waddell, W. J. (1956) *J. Lab. Clin. Med. 48*, 311–314.
Yao, J., Lowary, P. T., & Widom, J. (1991) *Biochemistry 30*, 8408–8414.